Journal of Computer-Aided Molecular Design, 11 (1997) 114–128
ESCOM

J-CAMD 383

Structure–affinity relationships for the binding of actinomycin D to DNA

José Gallego*,**, Angel R. Ortiz***, Beatriz de Pascual-Teresa**** and Federico Gago**

Department of Physiology and Pharmacology, University of Alcalá, E-28871 Alcalá de Henares, Madrid, Spain

Received 20 May 1996
Accepted 9 October 1996

Keywords: DNA intercalation; Actinomycin D; Stacking interactions; Electrostatic interactions

Summary

Molecular models of the complexes between actinomycin D and 14 different DNA hexamers were built based on the X-ray crystal structure of the actinomycin–d(GAAGCTTC)$_2$ complex. The DNA sequences included the canonical GpC binding step flanked by different base pairs, nonclassical binding sites such as GpG and GpT, and sites containing 2,6-diamino-purine. A good correlation was found between the intermolecular interaction energies calculated for the refined complexes and the relative preferences of actinomycin binding to standard and modified DNA. A detailed energy decomposition into van der Waals and electrostatic components for the interactions between the DNA base pairs and either the chromophore or the peptidic part of the antibiotic was performed for each complex. The resulting energy matrix was then subjected to principal component analysis, which showed that actinomycin D discriminates among different DNA sequences by an interplay of hydrogen bonding and stacking interactions. The structure–affinity relationships for this important antitumor drug are thus rationalized and may be used to advantage in the design of novel sequence-specific DNA-binding agents.

Introduction

The long-sought goal of achieving base-sequence specificity for DNA-binding agents implies having a detailed knowledge of the discriminating forces involved in the stabilization of the different possible complexes. Central to the recognition of a particular DNA sequence by antibiotics and other small ligands are the hydrogen bond donor and acceptor atoms in the minor groove of the double helix, which are usually considered to be the key elements for specificity. Thus, the N3 atoms of adenines and the O2 atoms of thymines are essential for the binding of distamycin-like compounds to A,T-rich regions whereas the 2-amino group of guanine is crucial for the recognition of guanine steps by actinomycin D or echinomycin-like antibiotics [1].

The clinical importance of actinomycin D (Fig. 1) and its marked preference for binding to guanosine residues in DNA [2] make this drug an attractive model for the study and design of new sequence-specific DNA-binding ligands. Its antineoplastic activity is thought to arise from its ability to block RNA synthesis by preventing the progression of the RNA polymerase along the DNA template, and a variety of biophysical methods have been used to gain insight into the structural, thermodynamic and kinetic aspects of actinomycin–DNA complex formation.

By subjecting DNA–actinomycin complexes to the action of reagents which degrade DNA, such as methidiumpropyl-EDTA·Fe [3] or DNase I [4–6], followed by electrophoresis of the DNA on a high-resolution polyacrylamide gel, sites protected by the antibiotic from cleavage show up as blank spaces on the autoradiograph of the gel. These 'footprinting' studies have demonstrated that 5'-GpC-3' (GpC) is the preferred binding site for actinomycin, although it can also bind to GpG (CpC) and, more weakly, to GpT (ApC) sequences [7,8]. The existence of these secondary binding sites has also been detected by equilibrium binding studies [9–11].

The first structural insight into the binding mechanism and the source of the specificity for guanine was provided

*Present address: Department of Chemistry, University of Washington, Seattle, WA 98195, U.S.A.
**To whom correspondence should be addressed.
***Present address: The Scripps Research Institute, La Jolla, CA 92037, U.S.A.
****Present address: Department of Chemistry, Universidad San Pablo CEU, E-28668 Madrid, Spain.

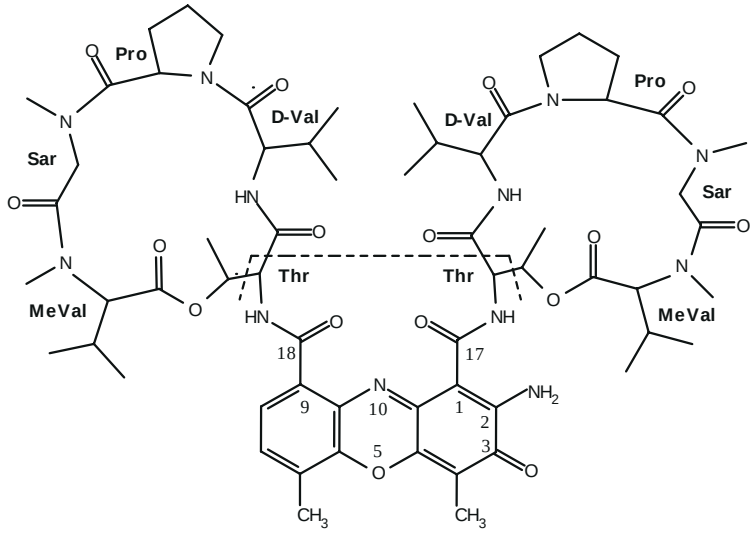

Fig. 1. Chemical structure of actinomycin D. The fragments used for energy decomposition, chromophore and depsipeptides, are separated by a dashed line. Atom positions relevant to the text have been numbered.

by a crystalline complex of actinomycin D and deoxyguanosine [12], which revealed strong hydrogen bonding interactions between the 2-amino group of guanine and the carbonyl oxygen of the threonine residues. Similar hydrogen bonds were later detected in the pseudo-intercalated complex of actinomycin with d(GpC) [13] and, more recently, in the complexes of actinomycin with the oligonucleotide $d(GAAGCTTC)_2$ in two different space groups [14,15]. These complexes have confirmed the validity of the models initially proposed [12,16], according to which the binding of actinomycin D to DNA involves intercalation of the 2-aminophenoxazin-3-one planar chromophore between two base pairs and fitting of the two cyclic pentadepsipeptides into the minor groove, each extending for two base pairs on either side of the intercalation site (Fig. 2).

The resolution of these structures strengthened the belief that the guanine–threonine hydrogen bonds are the factors responsible for the specificity of actinomycin binding to GpC steps, a hypothesis that was supported by theoretical studies [17]. Earlier reports, however, pointed to electronic interactions between the phenoxazone chromophore and the relatively polarized G:C base pair as the source of specificity for guanine over the other common bases. In fact, this specificity is retained in both actinomine, an actinomycin analogue in which the cyclic pentapeptides have been replaced by *N*,*N*-diethylethylen-diamine side chains, and 2-aminophenoxazin-3-one, neither of which can form hydrogen bonds with the 2-amino groups of guanine [2,18]. In line with these findings, proton magnetic resonance studies of complexes of actinomycin D with different mono- and dinucleotides demonstrated that the quinoid portion of the phenoxazone chromophore binds guanine nucleotides much more strongly than adenine nucleotides, whereas the benzenoid portion binds both guanine and adenine with the same affinity [19,20], a preference that cannot be accounted for by hydrogen bonding mechanisms. On the other hand, it is not straightforward for a hydrogen bonding probe to detect a base pair reversal in the minor groove, i.e. GpC

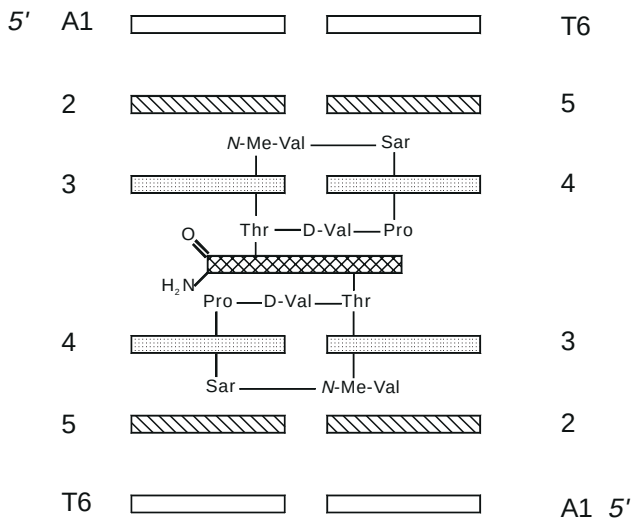

Fig. 2. Schematic representation of a complex between actinomycin D and a DNA hexanucleotide as seen from the major groove. The base pairs immediately adjacent to the intercalation site are named *central* pairs, and are dotted; the base pairs contiguous to these pairs are termed *flanking* pairs, and are hatched. Note that, whereas the central bases always have an acceptor atom for hydrogen bonding to the NH groups of the threonine residues, the presence of the 2-amino group for interacting with the carbonyl groups of these residues depends on base composition and sequence. For the asymmetric GpG (CpC), GpT (ApC) or ApA (TpT) central steps, the antibiotic was complexed in two alternative orientations: with the quinoid portion of the chromophore stacked between the purine bases in GpG and ApA or between G and T in GpT (a), or with the quinoid portion stacked between the pyrimidine bases in GpG and ApA or between A and C in GpT (b).

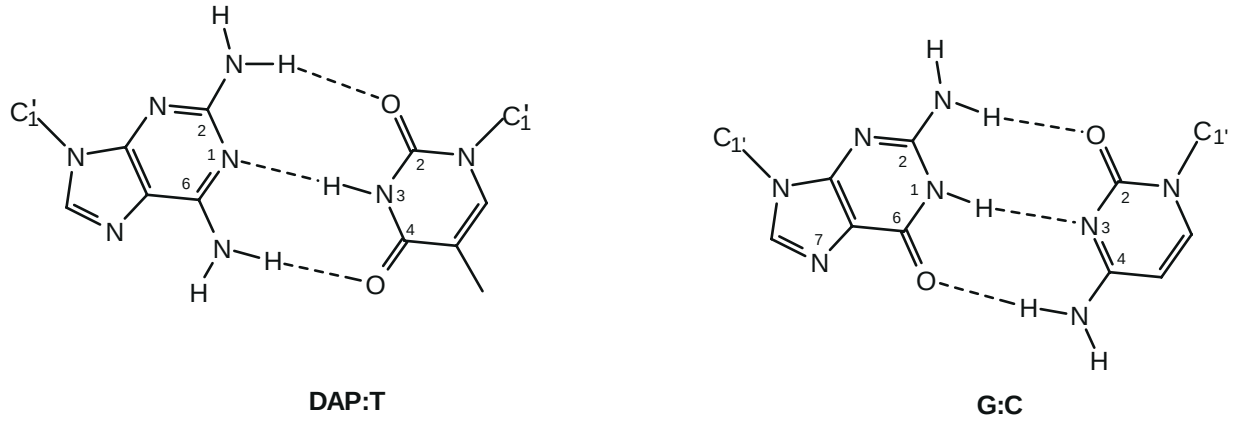

Fig. 3. DAP:T and G:C base pairs, both containing an exocyclic 2-amino group in the minor groove.

versus CpG, because the 2-amino groups of guanines occupy virtually equivalent positions in space in both steps [21]. This reasoning notwithstanding, some nonclassical binding sequences, like GpG (CpC) or GpT (ApC), must lack one guanine–threonine hydrogen bond, but nonetheless have been reported to be good binding sites for actinomycin [9–11].

The last piece of evidence that further suggests the intervention of additional elements of recognition apart from the hydrogen bonds comes from experiments in which nonstandard bases have been incorporated into the DNA molecule. Early assays had already shown that actinomycin was able to bind to an alternating sequence of dDAP (DAP = 2,6-diamino-purine) and dT [22], but recent footprinting experiments have demonstrated that when DAP (D) substitutes for adenine in a *tyr*T DNA fragment, the sequence specificity of actinomycin is drastically altered, and the drug binds to any 5'-purine-pyrimidine-3' (RpY) step different from the standard GpC site [23]. Since the minor grooves of the GpC and DpT steps present similar hydrogen bonding capabilities (Fig. 3), this interaction cannot adequately explain the observed change in binding preferences.

As regards the base pairs *flanking* the dinucleotide intercalation step, equilibrium binding and kinetic studies have shown that they modulate the binding affinities of the drug for GpC sites [10,24,25]. Footprinting techniques have also been used to measure the binding constants and kinetics of dissociation from individual sites [8]. In general, pyrimidines are preferred over purines on the 5' side of the GC doublet, and GGCC is particularly disfavored (Table 1).

In order to gain a more detailed understanding of the interactions that govern the sequence-specific binding of actinomycin to DNA, we have built molecular models of 14 double-helical DNA hexamers in which the drug intercalates at the central dinucleotide step (Fig. 2). The complexes can be grouped into three different categories. A first family of seven sequences contains ApApXpZpTpT as the basic unit, where the central XpZ step is either the canonical GpC step, a secondary GpG (CpC) or GpT (ApC) site, or any of the nonpreferred sequences, CpG, ApT, ApA (TpT) and TpA. In order to assess the influence of the flanking base pairs on the binding of actinomycin to GpC, a second subset of ApXpGpCpZpT sequences was built, where the canonical central step is conserved and the X--Z combinations are T--A, G--C and C--G. The last family comprises four modified DNA sequences of general formula DpXpDpTpZpT, in which a nonstandard DpT step is flanked by all possible X--Z combinations in the modified *tyr*T DNA fragment, i.e. D--T, T--D, G--C and C--G. For the asymmetric sequences GpG (CpC), GpT (ApC) and ApA (TpT), the antibiotic was studied in two alternative orientations, called

TABLE 1
EXPERIMENTALLY DETERMINED SELECTIVITY OF ACTINOMYCIN D BINDING TO DIFFERENT DNA DINUCLEOTIDES[a] (1) AND TO GpC DINUCLEOTIDES FLANKED BY DIFFERENT BASE PAIRS[b] (2)

(1)	DpT > GpC > GpG (CpC) > GpT (ApC) ≫ CpG, ApT, ApA (TpT), TpA
(2)	TGCA [–9.4] > CGCG [–9.2] > AGCT [–8.9] ≫ GGCC [–7.1]

[a] At the dinucleotide level, DpT is the maximum affinity DAP-containing binding site, GpC is the preferred natural step, and GpG and GpT are secondary binding sites. There is no appreciable binding to the remaining dinucleotides. This binding profile has been deduced mostly from footprinting experiments [7,8,23].

[b] Binding constants (T = 18.5 °C) reported for these sequences [24] have been transformed into binding free energies (numbers in brackets, kcal mol^{-1}) by using the relationship $\Delta G° = -RT \ln K_a$. Additional thermodynamic binding data are available for several other non-self-complementary sequences [8,10,11,25], but they are lacking for the remaining sequences studied here including those containing a central nonstandard DpT site. For greater ease of interpretation, our study was centered on symmetric sequences, most of them self-complementary (Fig. 4).

a and b (see the legend to Fig. 2). Thus, a total of 17 complexes (hereafter referred to by their central tetranucleotide) containing every combination of YpR and RpY binding sites experimentally probed by actinomycin were built. The whole set contemplates all possible hydrogen bonding arrangements between the depsipeptides and the DNA atoms in the minor groove as well as all possible combinations of stacking interactions. The complexes were energy refined and the intermolecular interaction energies were partitioned into different van der Waals and electrostatic components. The resulting data matrix was subjected to principal component analysis as a means to highlight the structure–affinity relationships (SAR) for this important antitumor antibiotic.

Methodology

Model building and energy refinement

The crystal structure of the complex between actinomycin D and d(GAAGCTTC)$_2$ [15], retrieved from the Brookhaven Protein Databank [26], was used as a template in the construction of the complexes studied. Of the three structures reported for this complex in two different space groups, the one crystallized in space group F_{222} and labeled *A* by Kamitori and Takusagawa [15] was chosen. This complex displays twofold symmetry around the N10-O5 axis in the phenoxazone ring, and the same interring hydrogen bonds between the D-valine residues of the pentapeptides detected in the structures of isolated actinomycin [27] and in all of the actinomycin–DNA structures except for the F_{222} complex *B* [15]. When the calculations detailed below were carried out on complex *C*, which is an intermediate between complexes *A* and *B* crystallized in space group C_2 [14], similar results were obtained [28].

For the DNA hexamers, the appropriate modifications of base composition were introduced by replacing the respective purine and pyrimidine bases where necessary, using standard geometries [29]. The initial conformation of the antibiotic in all the complexes was that found in the crystal structure. Ten counterions resembling hexahydrated sodium ions were then placed in the bisector of each O-P-O group in order to achieve electroneutrality [30].

The AMBER all-atom force field parameters [29] were used for the standard DNA molecules. Additional parameters for DAP have already been reported [31]. The equilibrium bond lengths and angles of the actinomycin chromophore were obtained by averaging over five crystal structures [13,14,27,32]. The corresponding force constants were derived by interpolation (distances) or by analogy (angles) [33].

The C1-C17 and C9-C18 bonds of actinomycin D (Fig. 1) link the phenoxazone system to the cyclic depsipeptides and therefore govern the relationships among these three essentially rigid moieties of the antibiotic [27], and hence their interactions with DNA [15]. Due to the possible importance of this pivotal role, a careful parameterization of the corresponding torsional potential was undertaken by using the method of Hopfinger and Pearlstein [34].

In order to obtain an accurate representation of the electrostatic charge distribution, the molecular electrostatic potential (MEP) was calculated from the corresponding wave functions using the AM1 Hamiltonian [35]. For this purpose, *N*,*N*-dimethyl(4,6-dimethyl-2-aminophenoxazin-3-one)1,9-dicarboxamide (hereafter named phenoxazone-1,9-dicarboxamide for simplicity) and the pentapeptide of actinomycin in the α conformation [14, 15] were used. For the subsequent energy analyses, the NH-C$^{\alpha}$ groups of the threonine residues were considered as part of the chromophore (Fig. 1). This is consistent with the method used for charge derivation, avoids splitting of the CO-NH carboxamide dipoles, and allows the charge of the chromophore to be neutralized by using the C$^{\alpha}$ atoms of the threonines as buffers. This latter point is particularly important for the calculation of electrostatic stacking interactions (see below). Moreover, this approximation does not bias the results, because the bases at the 5' side of the chromophore *always* present an acceptor atom, either N3 or O2, to form weak hydrogen bonds with the NH groups, irrespective of the binding sequence (Table 3).

Partial atomic charges were derived by fitting the MEP to a monopole–monopole expression according to the CHELP scheme [36], as implemented in the SPARTAN program [37]. For the graphical representation of the MEP shown in Fig. 9, the AM1 wave function [35] obtained for phenoxazone-1,9-dicarboxamide was used as input for the MEPMIN module of the MEPSIM program [38]. A cubic lattice was defined with a spacing of 1.0 Å in the x and y directions, which define the plane of the rings, and 0.5 Å in the z direction, and the MEP was calculated at each point. The resulting MEP values were read in by the *contour* facility of INSIGHT II [39] and displayed as a colored map-plane.

The initial model complexes were refined by progressively minimizing their potential energy [29]: firstly counterions and hydrogen atoms only, then the central tetranucleotides of the DNA hexamers, and finally the complete systems. Before the latter two minimization stages, a short optimization run, restraining all non-H ligand and DNA atoms to their initial coordinates, allowed a readjustment of covalent bonds and van der Waals contacts without changing the overall conformation of the complexes. All atom pairs were included in the calculation of the nonbonded interactions. The optimizations were carried out in a continuum medium of relative permittivity $\varepsilon = 4r_{ij}$ for simulating the solvent environment. For the first 3000 steps of the minimization procedure, all possible hydrogen bonds between the threonine residues and suitable donor and acceptor atoms at the bottom of the minor groove, together with the hydrogen bonds between

the DNA base pairs, were reinforced with distance and angle restraining functions with force constants of 10 kcal mol^{-1} $Å^{-2}$ and 10 kcal mol^{-1} rad^{-2}, respectively. The complexes were then subjected to *unrestrained* minimizations until the root-mean-square difference (rmsd) of the derivatives of the potential energy with respect to the atomic coordinates was less than 0.05 kcal mol^{-1} $Å^{-1}$. All in all, the optimizations covered a total of about 6000 steps of steepest descent energy minimization for each of the complexes. The average rmsd for all non-H atoms between the initial and minimized structures was 0.82 ± 0.02 Å. All programs were run on a Control Data Cyber 910 workstation.

Partial atomic charges and bonded and nonbonded parameters for the actinomycin residues are available from the authors on request.

Analysis of electrostatic interactions

The electrostatic energy of interaction between two groups of M and N atoms is described (in kcal mol^{-1}) by the Coulomb equation:

$$E_{el} = 332 \sum_{i=1}^{M} \sum_{j=1}^{N} \frac{q_i q_j}{\varepsilon r_{ij}} = 332 \sum_{i=1}^{M} q_i \sum_{j=1}^{N} \frac{q_j}{\varepsilon r_{ij}} = 332 \sum_{i=1}^{M} q_i \phi_i \quad (1)$$

where q represents the atomic point charges, r is the separation among them, ε is the relative permittivity of the medium, and ϕ_i is the electrostatic potential at each of the M atoms of the first group due to the N atoms of the other group. A distance-dependent dielectric model, while useful for dampening electrostatic interactions during the refinement stage, does not take into account the effect of the discontinuity between the low dielectric solute and the high dielectric solvent, which may also contain salt [40]. Consequently, in our analysis of electrostatic interactions ϕ_i was obtained by solving the linear form of the Poisson–Boltzmann equation:

$$\nabla[\varepsilon(\vec{r}) \nabla \phi(\vec{r})] = -4\pi\rho(\vec{r}) + \bar{\kappa}^2 \phi(\vec{r}) \quad (2)$$

where ρ is the fixed solute charge distribution and $\bar{\kappa}$ accounts for a Boltzmann distribution of the ions in solution. The finite difference method of Klapper et al. [41] was used, as implemented in the DelPhi module of INSIGHT II [39]. Solvent-accessible surface areas were calculated by means of a spherical probe of 1.8 Å radius representing a water molecule [42], and the solute and solvent phases were assigned dielectric constants of 2 and 80, respectively. The ionic strength of the solvent was 0.145 mol l^{-1}, a value comparable to those used in the majority of the experiments [10,11,24,25]. The ion radius for the Stern layers was 2 Å. A grid was superimposed on the molecule and the electrostatic potential was calculated at each grid point, using a focusing method [43] to optimize the boundary conditions of the grid. The focused calculations were carried out on 2 point $Å^{-1}$ grids, and the values for ϕ_i were obtained by interpolating from the surrounding grid points. The actinomycin and DNA atoms were assigned the same charges and van der Waals radii as those employed in the molecular mechanics force field, except for the charges of the C1' atoms of the DNA nucleosides and the C^{α} atoms of the threonine residues of actinomycin. These atoms were used as buffers when necessary in order to achieve electrical neutrality for the DNA base pairs and the actinomycin chromophore, respectively [31].

It is important to realize that the energy of any possible intermolecular hydrogen bonds will be implicitly accounted for in the Poisson–Boltzmann calculations.

TABLE 2
INTERACTION ENERGY VARIABLES[a] USED IN THE PCA

	Central base pairs		Flanking base pairs	
	Electrostatic	van der Waals	Electrostatic	van der Waals
Chromophore	**1**	**5**	**2**	**6**
Depsipeptides	**3**	**7**	**4**	**8**

[a] The antibiotic and DNA fragments are defined in Figs. 1 and 2.

Principal component analysis

The energy of interaction between actinomycin and each of the DNA hexamers was dissected by dividing the antibiotic into two fragments, the chromophore and the depsipeptides (Fig. 1), and considering the central and the flanking base pairs of the DNA hexanucleotides separately (Fig. 2). For each interaction, a 6-12 van der Waals term, as implemented in AMBER, and a Poisson–Boltzmann electrostatic term were computed (Table 2). This procedure yielded eight variables per complex, i.e. a data matrix of 17 rows and 8 columns, which was subjected to principal component analysis (PCA) [44] using the NIPALS algorithm [45].

PCA is a statistical multivariate technique that extracts the maximum amount of common information from a data matrix by defining a smaller number of uncorrelated new variables (*principal components*) that explain most of the variation contained in the original matrix. The essential data patterns can be easily visualized by plotting the complexes in the space of the principal components (*score plot*), whereas the relation between original and new variables can be unveiled by plotting the contributions of the variables to each principal component (*loading plot*).

Evaluation of the hydrogen bonding geometries

The orientation of the donor-hydrogen-acceptor and acceptor-lone pair-hydrogen systems in the refined complexes was taken into account in order to assess the quality of the hydrogen bonds between actinomycin and DNA. To this end, a factor (h) was calculated that corresponds to the product of the Ep and Et functions of Boobyer et al.

[46], developed by fitting to experimental hydrogen bonding geometries. h varies from 0 (no bond) to 1 (ideal bond).

Results

Correlation of calculated actinomycin–DNA interaction energies with experimental binding preferences

The calculated interaction energies (Fig. 4) reflect well the relative affinities [7,8] of actinomycin D for the different sites (Table 1): the canonical GpC step is energetically favored over any other central step in the first family of natural sequences, followed by GpG (CpC) and GpT (ApC), which are known to be secondary binding sites [7,8]. In the second group of complexes, pyrimidines are indeed preferred over purines on the 5' side of the GpC intercalation site, with GGCC appearing as the least favored sequence [5,8,24]. Furthermore, the most favorable binding energies in the whole set are those belonging to sequences in which the adenines have been replaced with DAP, in accord with recent experimental results showing that these sites are protected from DNase cleavage more efficiently than standard GpC steps [23].

Interplay of hydrogen bonding and stacking interactions in the association of actinomycin D with DNA

In order to identify the energy components involved in sequence discrimination, the overall interaction energies were decomposed into van der Waals and electrostatic contributions from either the phenoxazone-1,9-dicarboxamide system or the depsipeptides of the drug and the DNA base pairs that either make up or flank the intercalation site (Table 2). From the resulting matrix of 17 complexes and 8 interaction energy variables, the first two principal components (PC1 and PC2) were found to readily explain 90.1% of the variance contained in the original data matrix and to reproduce remarkably well the experimentally observed sequence preferences of actinomycin D (Fig. 5a). The different clusters of sites are easily discriminated along the horizontal axis (PC1). There is not a single violation in the ranking of the complexes (cf. Table 1), from the most favored DAP:T sequences (left) to the most disfavored A:T-containing sites (right), going through the classical GpC steps and the secondary GpG and GpT sites. As can be seen by the loadings in Fig. 5b, the highest coefficients that make up PC1 come from the electrostatic interactions of the peptides with the central base pairs (variable **3**, which includes the sequence-dependent part of the hydrogen bonding energy), and the van der Waals and electrostatic interactions of the chromophore with the same base pairs (variables **5** and **1**, respectively). Thus, actinomycin D can discriminate among the different sequences by an *interplay* of hydrogen bonding and stacking interactions. Each of these contributions will now be separately analyzed.

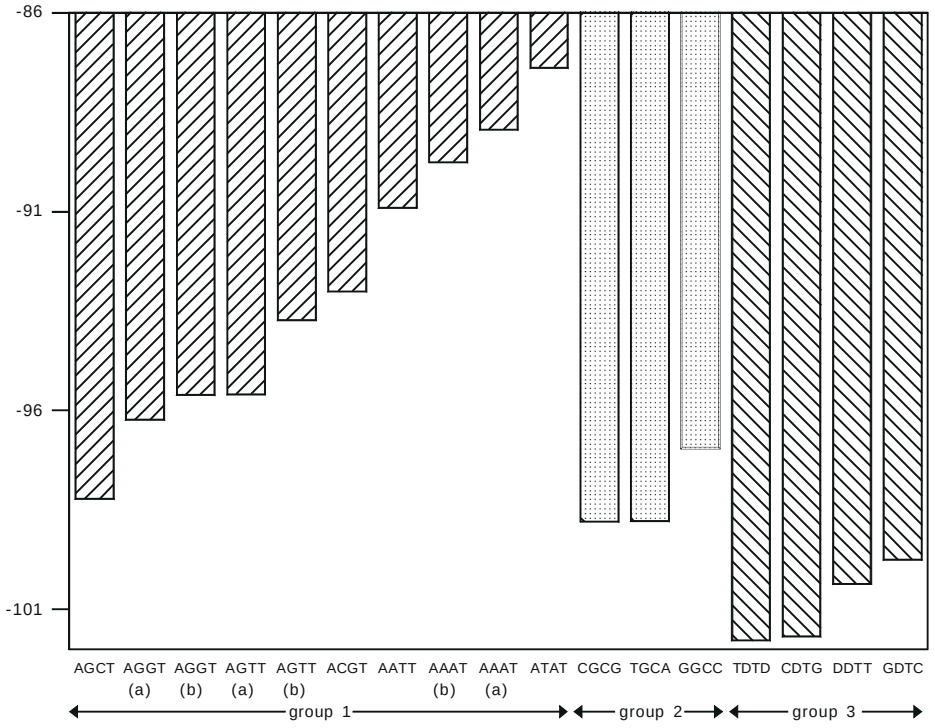

Fig. 4. Total interaction energies (kcal mol^{-1}) between actinomycin and the DNA hexamers. For each family of sequences, the complexes are ordered by decreasing interaction energies. These values were calculated by adding the AMBER 6-12 van der Waals term to the electrostatic interaction energies obtained by solving the Poisson–Boltzmann equation. Calculation of the total interaction energies using the AMBER force field with a relative permittivity of $\varepsilon = 4r_{ij}$ yielded the same relative results. The different oligonucleotides are identified by the central four bases of one strand in the 5'→3' direction.

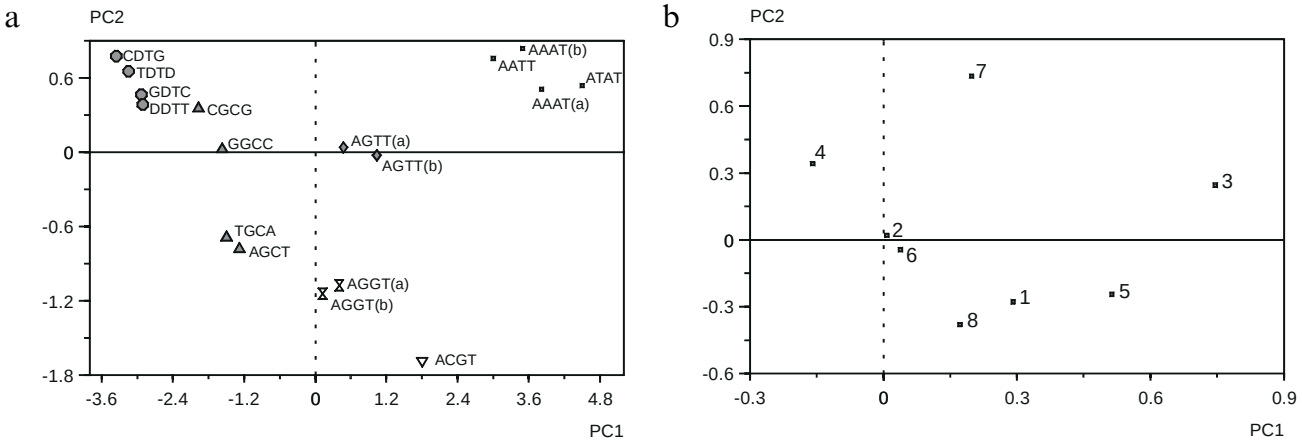

Fig. 5. (a) Scores and (b) loadings from a PCA of the van der Waals and electrostatic interaction energies between the chromophore and the depsipeptides of actinomycin and the central and flanking base pairs of the whole set of DNA hexamers studied (cf. Table 2). A more detailed analysis considering the chromophore, each of the pentapeptides, and each of the four base pairs separately, i.e. 24 interactions per complex, yielded similar results, as did an additional PCA performed after autoscaling the energy variables (data not shown). The independence of the results with respect to the definition of the fragments and the autoscaling procedure indicates that they are not strongly dependent on the methods used for modeling the complexes or analyzing the interactions.

Electrostatic interactions between the peptides and the central base pairs

The electrostatic interaction between the depsipeptides and the central DNA base pairs (variable **3**), which includes the intermolecular hydrogen bonds established by the carbonyl groups of the threonine residues, appears as the dominant factor for *overall* sequence selectivity, since the loading of this energy component to PC1 is the highest of all (Fig. 5b).

TABLE 3
GEOMETRICAL ANALYSIS OF HYDROGEN BONDS

Step	NH-N3/O2		CO-HN2	
	r[a]	h[b]	r[a]	h[b]
TpA	1.95 ± 0.02	0.47 ± 0.13	–	–
ApA (a)	2.01 ± 0.05	0.37 ± 0.01	–	–
ApA (b)	2.08 ± 0.18	0.40 ± 0.24	–	–
ApT	2.13 ± 0.10	0.30 ± 0.09	–	–
CpG	2.07 ± 0.09	0.35 ± 0.25	2.27 ± 0.16	0.27 ± 0.09
GpT (a)	2.13 ± 0.11	0.33 ± 0.13	1.95	0.69
GpT (b)	2.14 ± 0.01	0.27 ± 0.01	1.97	0.58
GpG (a)	2.05 ± 0.02	0.33 ± 0.14	2.20 ± 0.34	0.46 ± 0.36
GpG (b)	2.13 ± 0.05	0.32 ± 0.11	2.07 ± 0.11	0.43 ± 0.13
GpC[c]	2.15 ± 0.05	0.30 ± 0.06	1.96 ± 0.02	0.61 ± 0.06
DpT[d]	2.13 ± 0.05	0.31 ± 0.05	1.95 ± 0.01	0.65 ± 0.04

The hydrogen bonds listed are those between the NH groups of the threonine residues of actinomycin and the N3 or O2 atoms of the bases in position 5' with respect to the chromophore (NH-N3/O2), and between the carbonyl groups of the threonines and the 2-amino groups of the purines in position 5' or 3' with respect to the chromophore (CO-HN2). The interpeptide hydrogen bonds between the NH and CO groups of the D-valine residues [15,27] are maintained in all the complexes (data not shown). The 2-amino substituent on the phenoxazone chromophore forms a weak hydrogen bond with the O1' atom of the nearby deoxyribose in all the complexes (r = 2.25 ± 0.06 Å). The 1,9-carbonyl groups of the phenoxazone chromophore do *not* form hydrogen bonds (h = 0 in all the complexes), but are engaged in important electrostatic interactions (see text).

[a] r is the distance (Å) between the hydrogens and the acceptor atoms, averaged over the bonds from each half of the complex.

[b] The h factor depends on the orientation of the donor–H–acceptor and acceptor–lone pair–H systems (see the Methodology section), and is also averaged.

[c] Averaged over TGCA, AGCT, CGCG and GGCC.

[d] Averaged over TDTD, DDTT, CDTG and GDTC.

In order to assess whether the antibiotic is capable of recognizing base pair reversals through hydrogen bonding interactions (e.g. GpC versus CpG), we have estimated the distance and angle penalties for the actinomycin–DNA hydrogen bonds in the different complexes (Table 3). The carbonyl groups of the threonine residues appear to be capable of forming hydrogen bonds with the 2-amino groups on the central base pairs, irrespective of the position (5' or 3') of the purine base relative to the chromophore. In the ACGT complex, for example, the CO-HN2 distances denote hydrogen bonding, although the angle penalties are more severe than for the GpC steps (Table 3). Nevertheless, the interaction energies shown in Fig. 6 leave little room for doubt about the discriminative power of the electrostatic interactions between the peptides and the central bases. Adenine-containing steps, which lack the 2-amino groups in the minor groove and therefore cannot form any hydrogen bonds with the carbonyl groups of the threonine residues, are greatly disfavored. Different guanine-containing sites can also be distinguished on the basis of these interactions (compare, for example, the energy values for the GpC, GpG and CpG steps). The O^{γ} atoms of the threonine residues, which point toward the DNA minor groove, can also contribute to these relative differences.

Stacking interactions

The van der Waals and electrostatic components of the stacking interactions between the phenoxazone system and the central base pairs also contribute to the

DNA binding specificity (Fig. 5b), and are in fact crucial for the discrimination of some sequences. When the A:T-containing steps are excluded from the PCA, the relative importance of these forces (variables **5** and **1**) is more patent and their loadings equal that of the peptide interactions (Figs. 7a and b). Furthermore, these stacking interactions become the dominant factor for distinguishing between the GpC and DpT steps (Figs. 7c and d). Indeed, the electrostatic and van der Waals interaction energies between the phenoxazone-1,9-dicarboxamide chromophore and the adjacent base pairs can, on their own, account for the binding preferences of this antibiotic. Thus, DpT, GpC, GpG (CpC) and GpT (ApC) appear, in this order, as the best binding sites for actinomycin D (Fig. 8), in agreement with the experimental evidence (Table 1).

The electrostatic term of the stacking energy also enables the antibiotic to distinguish between RpY steps and YpR steps, favoring the former. Two of the most striking results of the present analysis concern the discrimination against CpG steps, for which this interaction energy term is repulsive, and the overall preference for DpT steps, for which this contribution is most favorable (Fig. 8a). In this respect, it is of interest to recall that the experimentally observed DNA binding preferences of the bis-intercalator echinomycin [23] have also been rationalized in terms of differences in stacking interactions [31,47].

In contrast to the quinoxaline-2-carboxamide chromophores of echinomycin [47,48], the phenoxazone-1,9-dicarboxamide chromophore of actinomycin D does not have a marked dipolar charge distribution. Instead, the two carboxamide groups attached perpendicularly to the aromatic ring system, and in opposite orientations, give rise to two alternate negative and positive electrostatic potential regions above and below the plane of the chromophore (Fig. 9). Whereas the NH groups of these carboxamide moieties always interact favorably through weak hydrogen bonds with the acceptor atoms (N3 or O2) of the bases in position 5' with respect to the chromophore (Table 3), the corresponding carbonyl groups always interact unfavorably with the N3 or O2 atoms of the bases on the 3' side. These carbonyl groups have received little attention so far, but we believe they play an important role in dictating the sequence specificity of this antibiotic. The presence of an exocyclic 2-amino group in the minor groove counterbalances the repulsion between these groups and the N3 or O2 atoms of the bases located on the 3' side. The antibiotic is thus able to distinguish between purine bases containing 2-amino groups and bases lacking an amino group in the minor groove. Steps made up of only A:T pairs are thus disfavored by these repulsive forces (Fig. 8a).

As regards the van der Waals term (Fig. 8b), the situation is rather similar. A:T-containing dinucleotides present less surface area for overlapping with the drug chromophore and are hence disfavored. As before, RpY steps

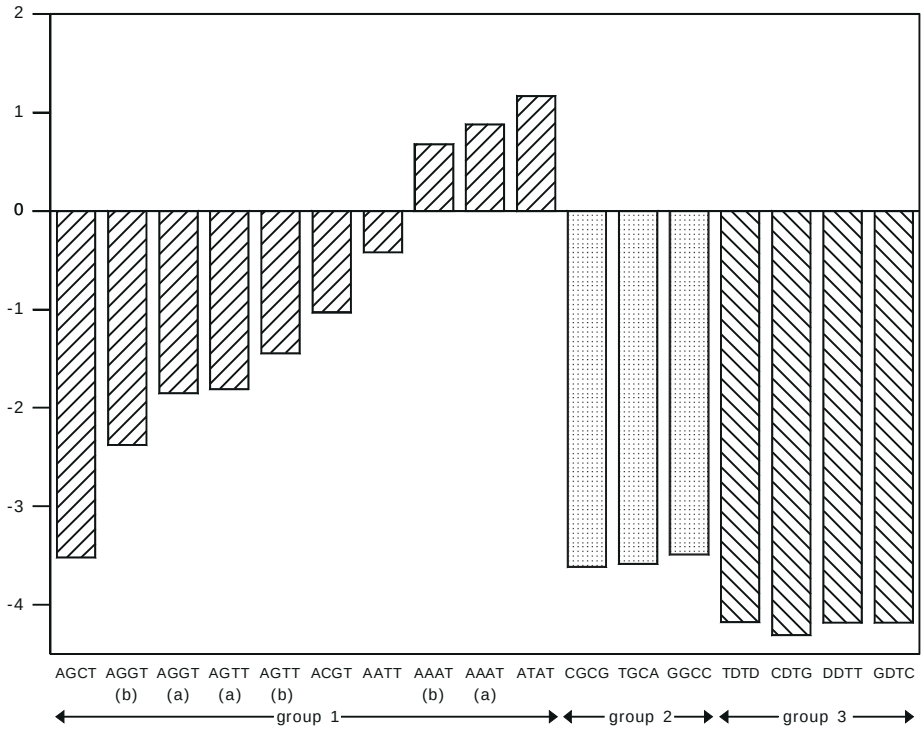

Fig. 6. Electrostatic interactions (kcal mol^{-1}) between the depsipeptide rings of actinomycin and the central DNA base pairs (energy variable **3**) in the different complexes studied. These values were calculated by solving the Poisson–Boltzmann equation and using the C1' atoms of deoxyriboses as buffers in order to achieve electroneutrality.

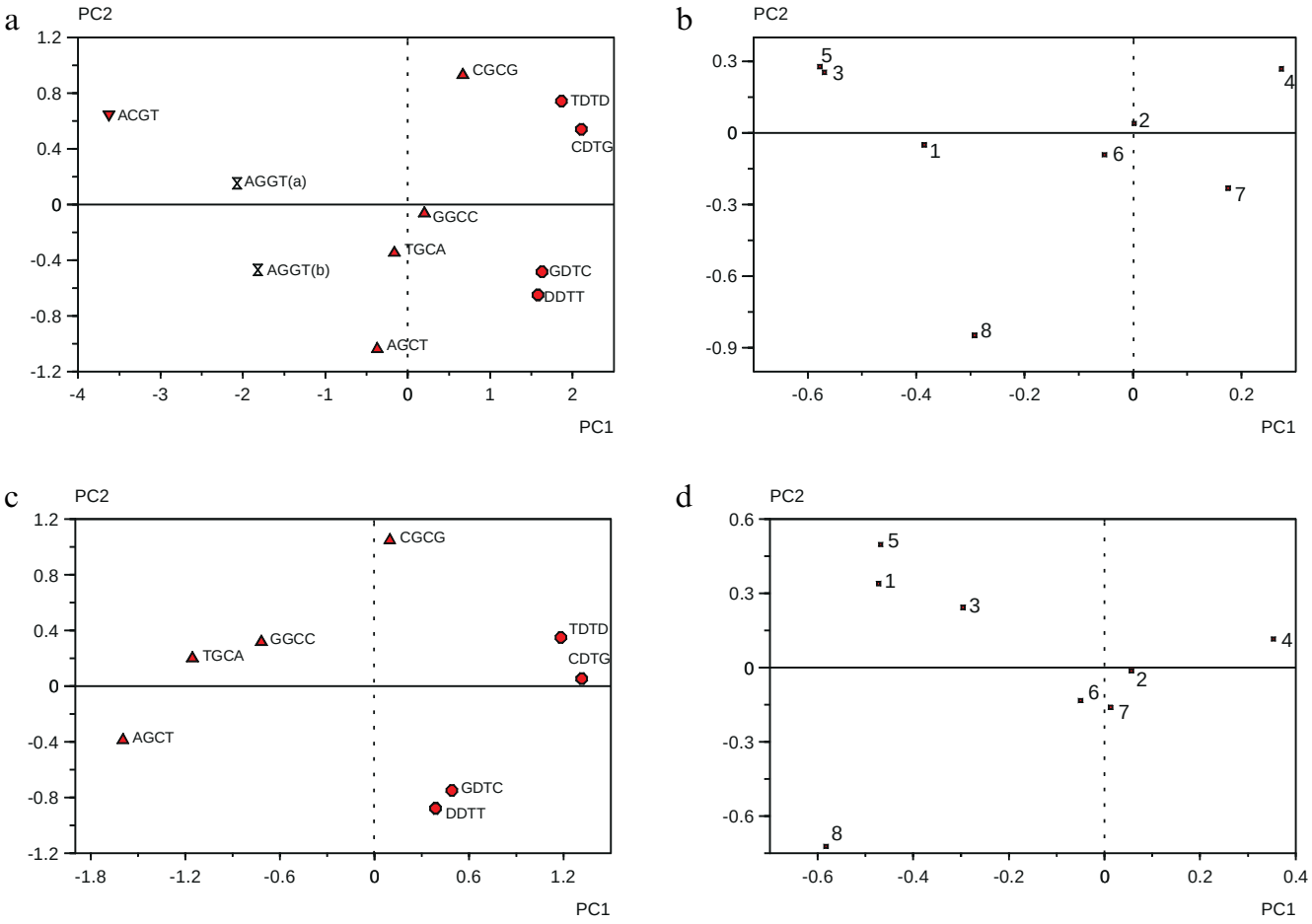

Fig. 7. (a) Scores and (b) loadings from a PCA of the van der Waals and electrostatic interaction energies between the chromophore and the depsipeptides of actinomycin and the central and flanking base pairs of only those DNA hexamers that contain guanine or DAP at both the central base pairs. (c) and (d) are the scores and loadings from a similar PCA including only the second and third families of complexes. The first two PCs explain 88.1% and 76.2% of the variance in (a, b) and (c, d), respectively.

are preferred over YpR steps, e.g. GpC versus CpG, and, again, a DpT step gives rise to better van der Waals stacking interactions than a GpC step.

Intercorrelation of the selectivity factors

The three selectivity factors unveiled in the present PCA, i.e. electrostatic interactions between the depsipeptide rings and the central bases (variable **3**), and van der Waals and electrostatic interactions between the phenoxazone ring system and the central bases (variables **5** and **1**) are correlated ($r_{3,5} = 0.952$; $r_{3,1} = 0.873$; $r_{5,1} = 0.925$), since they build into the same principal component (Fig. 5b). Physically, the reason is straightforward: if the central base pairs contain 2-amino groups, they are capable of forming hydrogen bonds with the threonine CO groups, and at the same time provide more overlapping surface area and give rise to better electrostatic interactions with the intercalating chromophore. These results reconcile different views on the relative importance of hydrogen bonding and stacking interactions in dictating the binding preferences of actinomycin D [12,18,19].

Interactions between the depsipeptide rings and the flanking base pairs

The electrostatic properties of the actinomycin pentapeptides (Fig. 10a) affect the interaction of the antibiotic with the base pairs that flank the intercalation site. By first focusing on the two principal components calculated for the complexes of the second and third families (Fig. 11), it can be seen that the electrostatic and van der Waals interactions between the depsipeptide rings and the flanking base pairs (variables **4** and **8**) are now the dominant discriminating factors (Figs. 11b and d). In the second family of complexes, two different clusters can be distinguished: on the one hand, complexes flanked by either G:C pairs (GGCC, CGCG) or A:T pairs (AGCT, TGCA) and, on the other hand, complexes having a purine (GGCC, AGCT) or a pyrimidine base (CGCG, TGCA) on the 5' side of the GpC step (Fig. 11a). How does the antibiotic discriminate between these two groups of complexes?

(1) GGCC and CGCG are distinguished from AGCT and TGCA by a combination of van der Waals and electrostatic terms operating in opposite directions (Fig. 11b).

As regards the electrostatic contribution, the more negative minor groove of an A:T pair relative to a G:C pair [49] gives rise to better electrostatic interactions with TGCA and AGCT than with CGCG or GGCC (Fig. 12a) because the dipole moment of each pentapeptide is directed toward the minor groove of the DNA molecule (Fig. 10a). On the other hand, the antibiotic appears to be able to accommodate 2-amino groups of purines in flanking positions, as suggested by Kamitori and Takusagawa [15], because the presence of these groups, rather than pushing the peptides away, improves the van der Waals interactions in CGCG and GGCC relative to TGCA and AGCT (Fig. 12b).

(2) GGCC and AGCT are distinguished from CGCG and TGCA primarily because of the van der Waals term (variable **8**). Thus, GpC steps flanked by pyrimidine bases in position 5' are favored by this energy component with

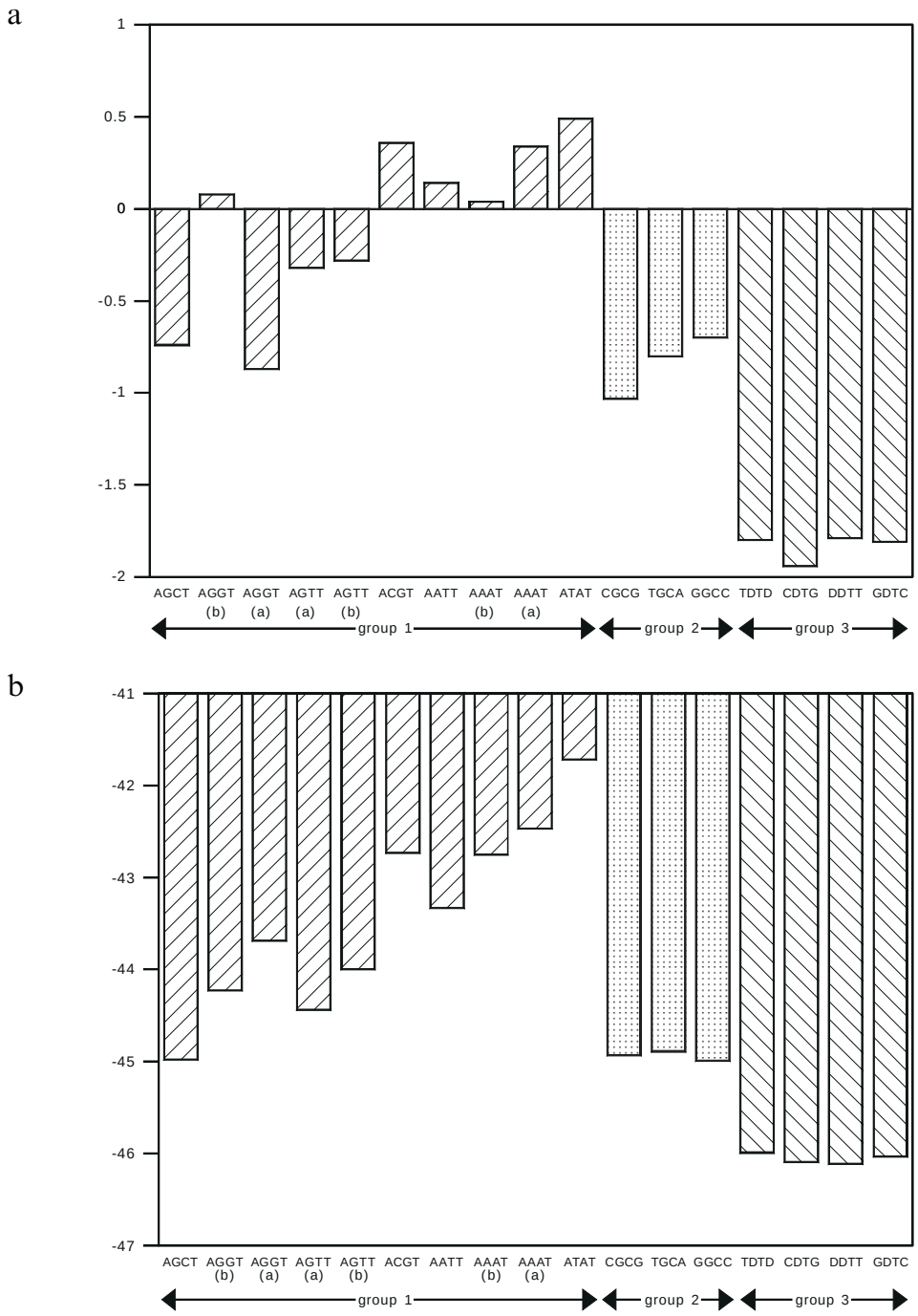

Fig. 8. (a) Electrostatic contributions (kcal mol^{-1}) to the stacking interaction energies between the *N*,*N*-C^{α}-phenoxazone-1,9-dicarboxamide chromophore of actinomycin D and the central base pairs (energy variable **1**) in the different complexes studied. These values were calculated by solving the Poisson–Boltzmann equation and using the C1' atoms of deoxyriboses and the C^{α} atoms of threonines as buffers in order to achieve electrical neutrality. (b) van der Waals contributions (kcal mol^{-1}) to the stacking interaction energies between the same groups (energy variable **5**).

respect to those flanked by purine bases in the same position (Fig. 12b).

The PCA on the third group of sequences (DDTT, TDTD, GDTC and CDTG) is characterized by the fact that in this case *every* base pair contains an exocyclic 2-amino group in the minor groove. Thus, DDTT and TDTD are distinguished from GDTC and CDTG (Fig. 11c) only by electrostatic interactions since only variables **4** and **2** significantly contribute to PC2 (Fig. 11d). The differences are smaller in this case because the minor groove has become less negative in all positions due to the presence of the 2-amino substituents (Fig. 12a). On the other hand, the discrimination between purine or pyrimidine bases on the 5' side of the DpT step remains evident (TDTD and CDTG versus DDTT and GDTC, Fig. 11c), and is almost exclusively due to a van der Waals effect (Figs. 11d and 12b), as was the case for the second group of sequences.

Compared to other sites containing a central GpC step, the GGCC sequence has been described as being particularly unfavorable for actinomycin binding [5,8,10,24]. In agreement with these results, our analysis identifies GGCC as the most disfavored sequence in the second family of complexes (Fig. 4) and pinpoints two possible sources of destabilization: (i) less favorable electrostatic interactions of the pentapeptides with the *flanking* G:C pairs (Fig. 12a); and (ii) less favorable van der Waals interactions with the same bases due to the presence of a purine base on the 5' side of the GpC step (Fig. 12b). The fact that footprinting and equilibrium binding studies relegate GGCC to the level of secondary sites such as GpC or GpT merits further study.

Discussion

In the present work, interaction energies were calculated between actinomycin D and a set of DNA hexamers representative of a variety of sites, both preferred for and excluded from drug binding. A SAR-type approach was then developed to identify the energy terms responsible for the sequence selectivity of the antibiotic. It should be pointed out that no account was taken of the conformational enthalpy changes undergone by either the drug or the DNA molecules upon binding. For actinomycin, these changes are small [14,15] and of similar magnitude for all the complexes considered (data not shown). On the other hand, an accurate estimation of the conformational energy changes in the DNA molecules is hampered by uncertainties regarding the sequence-dependent conformation of each DNA hexamer in the unbound state. Any enthalpic and entropic contributions of the solvent to the binding free energy other than those implicitly included in the Poisson–Boltzmann calculations have also been neglected. Thus, although the calculations focused on a partial aspect of the binding enthalpies, the ranking of the calculated interaction energies (Figs. 4 and 5a) is the same as the ranking of experimentally determined binding selectivities (Table 1).

In this regard, there is ample evidence that the initial unspecific binding of actinomycin D is followed by redistribution, or *shuffling*, to higher affinity sites along the DNA helix [50,51]. The long residence times that characterize optimal binding and determine the *specificity* of the drug could be directly determined by the actinomycin–DNA interaction energies, i.e. hydrogen bonding and stacking interactions. This should be particularly relevant for the selection of the *intercalation dinucleotide* step (Figs. 6, 8a and b).

As regards the selectivity of actinomycin D for DNA bases *adjacent* to the GpC intercalation step [10,24], the calculated interaction energies between the flanking base pairs and the peptidic part of the antibiotic (Fig. 12) also modulate the total interaction energies in a manner consistent with the differences in binding affinities (Table 1).

Actinomycin D is endowed with a high dipole moment ($\mu = 12.9$ D) whose positive pole points in the direction of the protruding chromophore (i.e. toward the DNA in the complex). We find this property to be shared with other DNA-binding antibiotics, like echinomycin ($\mu = 14.5$ D) and analogues (Fig. 10). The strong polarity of these antibiotics (for comparison, the dipole moment of a water molecule is 1.8 D) is due to the fact that almost all of the carbonyl groups of the depsipeptides (and also the sulfur atoms in echinomycin and triostin A) point away from the chromophore (i.e. toward the solvent in the complex), as described by other authors [14,52,53]. We suggest that this electrostatic asymmetry, already detected by Dean and Wakelin [52] for actinomycin D, aids in the approximation and correct orientation of the antibiotics with respect to the DNA molecule, perhaps compensating for the lack of net positive charge on these types of ligands.

The definite distribution of hydrophobic and polar groups in the actinomycin molecule may be relevant to the interactions of the drug with both the solvent and the DNA. Upon complex formation, the hydrophobic groups of proline, sarcosine and *N*-methyl-valine (Fig. 2) contribute to the desolvation of the DNA minor groove [14,15]. This release of water molecules has been suggested to contribute to the positive entropy changes detected for actinomycin binding to DNA [10,11,54], but it may also be disadvantageous for the binding enthalpies. This would explain why the binding to double-helical DNA of actinomine and analogues not possessing the depsipeptide rings of actinomycin [55], as well as the binding of actinomycin D to dGMP [55], is enthalpically more favorable than the binding of actinomycin D to most DNA duplexes [10, 11,54,55], in which parts of the minor groove will be desolvated.

It is of interest to note that if the electrostatic stacking energies obtained using the Poisson–Boltzmann method

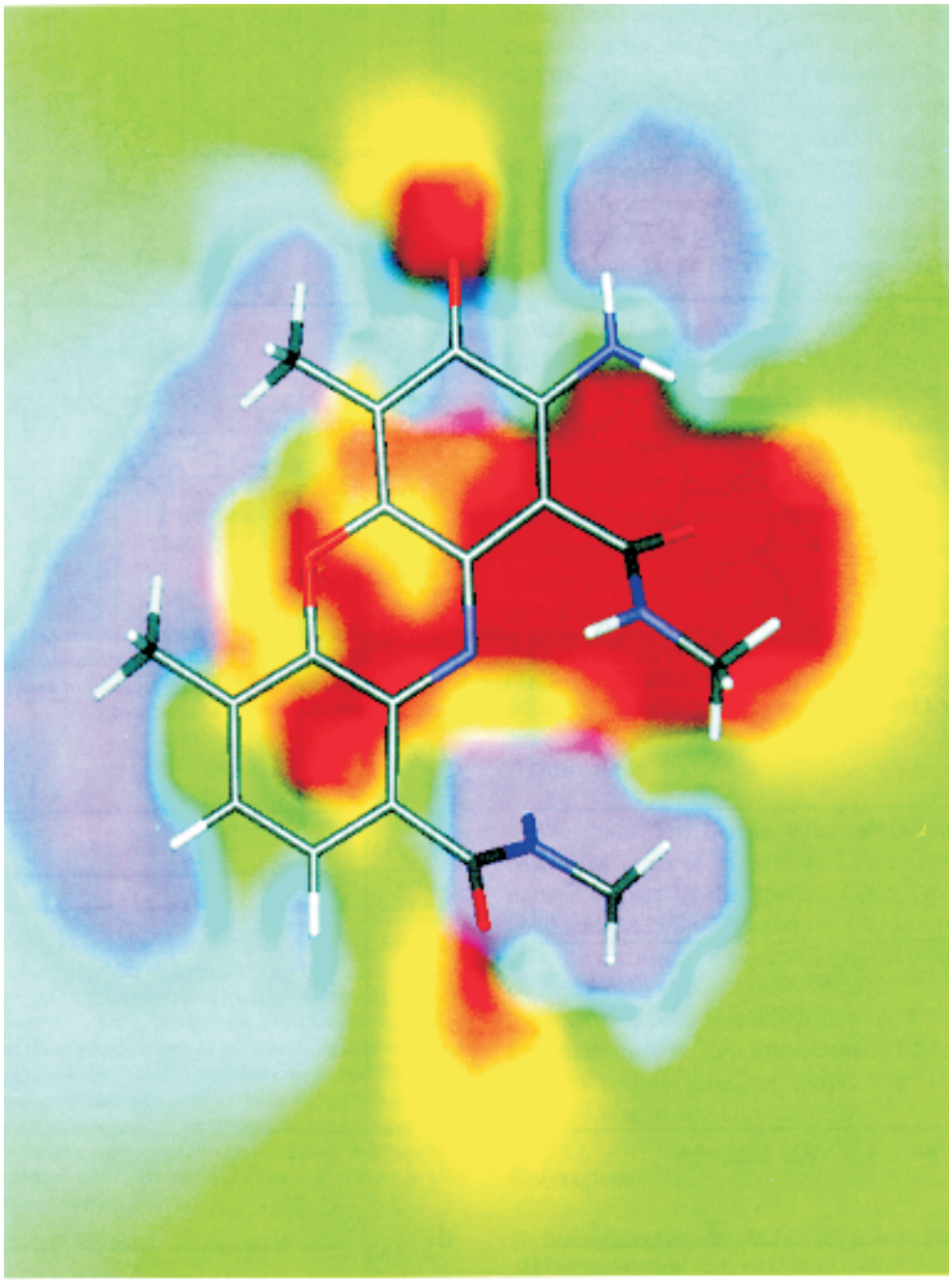

Fig. 9. Molecular electrostatic potential generated by the *N*,*N*-dimethyl(4,6-dimethyl-2-aminophenoxazin-3-one)1,9-dicarboxamide chromophore of unbound actinomycin D on a plane 1.7 Å *below* the atom centers, which approximates the recognition surface. The MEP is color-coded so that regions of 8 kcal mol^{-1} appear in blue and regions of –8 kcal mol^{-1} are colored in red, with intermediate values ramping smoothly; more positive and more negative regions are colored in violet and brown, respectively. C atoms are represented in gray, O atoms in red, N atoms in blue, and H atoms in white. Note that a MEP representation on a plane 1.7 Å *above* the atom centers will display an inversion of sign (colors) in the vicinity of the carboxamide CO and NH groups.

are compared with those calculated using the classical point charge approach with $\varepsilon = 1$, a good correlation is obtained ($r = 0.942$), and the effective dielectric constant [40] for these interactions turns out to be close to 2, the value that was used for the dielectric of the solute phase in the Poisson–Boltzmann calculations (see the Methodology section). This indicates that in actinomycin–DNA complexes these interactions are not affected by the reaction field of the solvent, most likely due to the 'umbrella' effect of both the depsipeptides in the minor groove and the protruding methyl groups of the chromophores in the major groove [14]. The resulting desolvation of these regions thus enhances actinomycin's discrimination of base composition and sequence based on electrostatic interactions.

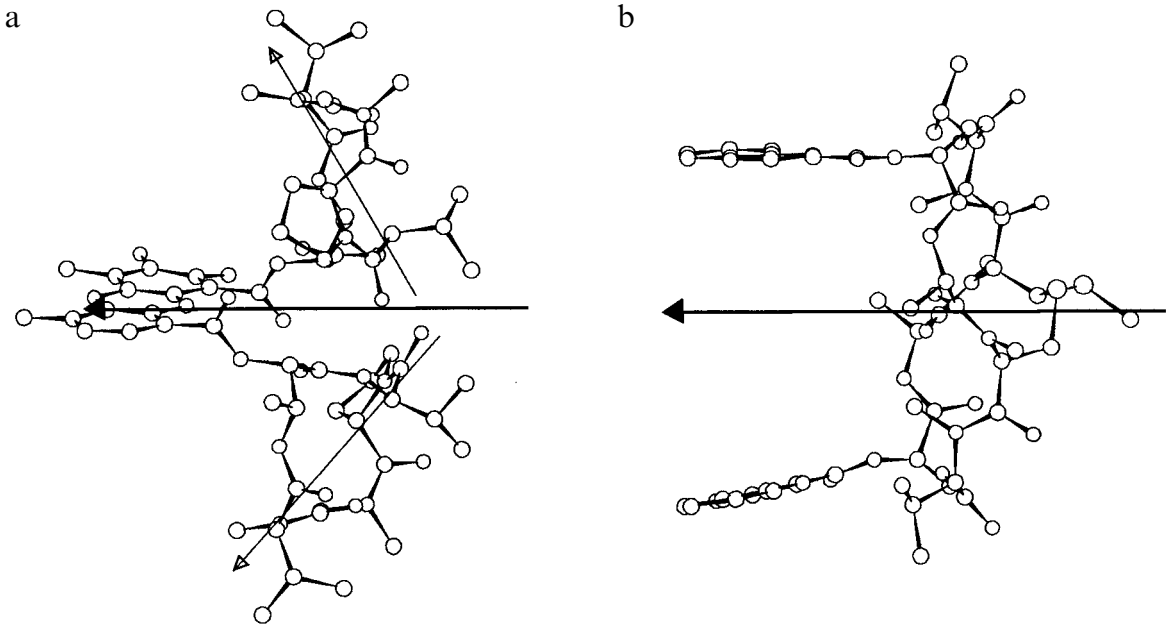

Fig. 10. Three-dimensional structures of (a) actinomycin D and (b) echinomycin showing the dipole moments (thick arrows) originating from the charge distribution of the whole molecules: 12.9 D for actinomycin and 14.5 D for echinomycin. Note that the arrowheads (positive pole) point to the site of interaction with DNA. Hydrogen atoms are not shown for clarity. For actinomycin, the dipole moment of each pentapeptide is also shown (thin arrows). The midpoint of each vector is centered on the geometrical center of the system considered.

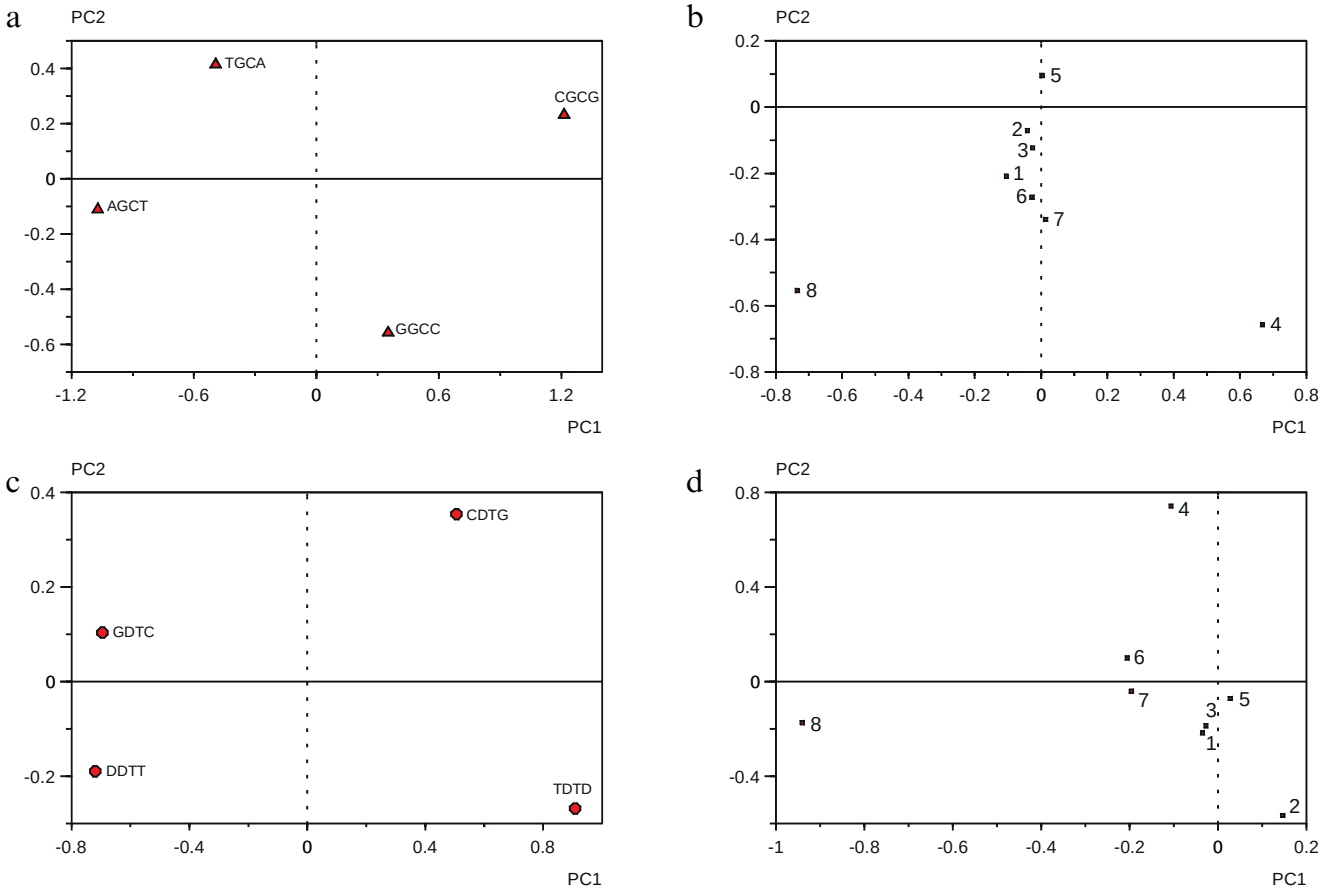

Fig. 11. (a) Scores and (b) loadings from a PCA of the van der Waals and electrostatic interaction energies between the chromophore and the depsipeptides of actinomycin D and the central and flanking DNA base pairs of the second family of complexes. (c) and (d) are the scores and loadings from a similar PCA carried out on the third family of complexes. In both cases, the first two PCs explain 96.2% of the variance.

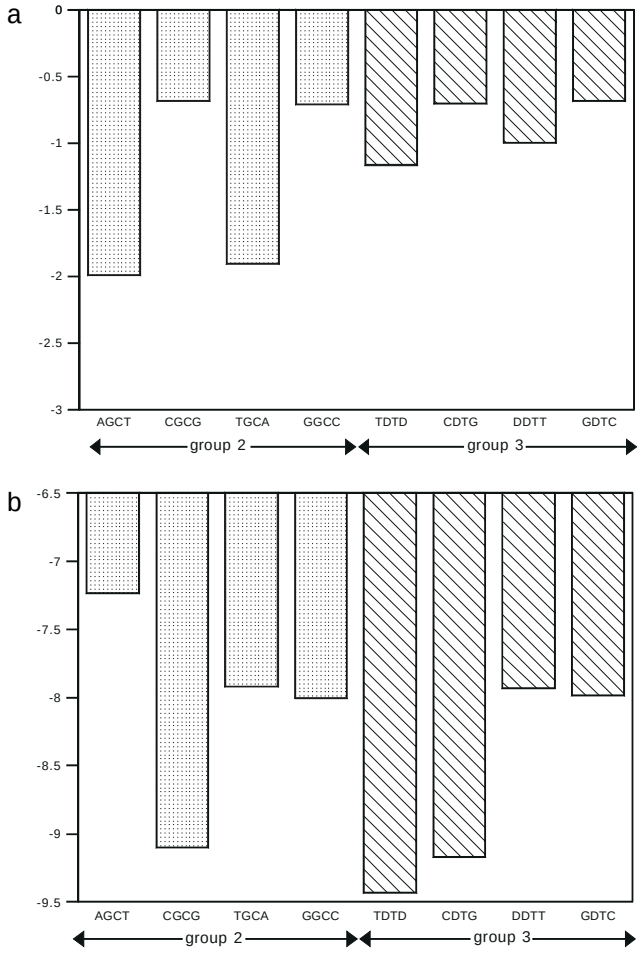

Fig. 12. (a) Electrostatic interaction energies (kcal mol^{-1}) between the depsipeptide rings of actinomycin and the flanking base pairs in the complexes of the second and third families (energy variable **4**). These values were calculated by solving the Poisson–Boltzmann equation and using the C1' atoms of deoxyriboses as buffers in order to achieve electrical neutrality. (b) van der Waals interaction energies (kcal mol^{-1}) between the same groups of atoms (energy variable **8**). In both groups of complexes, proline, sarcosine and *N*-methyl-valine were the peptide residues responsible for the differences in van der Waals interaction, whereas threonine and D-valine gave rise to similar interactions in all the complexes (data not shown).

Conclusions

We have found a good correlation between actinomycin–DNA interaction energies, calculated for a representative set of DNA hexamers containing standard and non-standard bases, and a number of experimental selectivities. A principal component analysis of the different energy contributions has shown that actinomycin D can discriminate among the different sequences by an interplay of hydrogen bonding and stacking interactions. Whereas the electrostatic and hydrogen bonding interactions of the peptides dominate the discrimination between G:C- and A:T-containing sites, in agreement with other authors [17], the importance of the stacking term increases for distinguishing amongst G:C-containing sites, such as GpC, GpG and CpG. The stacking interactions become crucial for favoring DpT over GpC central steps.

These results indicate that the presence of the 2-amino groups not only alters the hydrogen bonding potential or the geometry of the minor groove [1,56], but also imparts distinct stacking properties to the base pairs, both on steric and electrostatic grounds [47]. The intercalating ring is thus shown to participate in the binding specificity of actinomycin D, as previously suggested [2,18,19]. In this regard, stacking interactions between DNA bases and either neighboring bases or intercalating chromophores have also been shown to lead to strong conformational preferences [48,57,58] and to the preferential binding of other ligands to particular DNA sequences [31], even in the absence of any hydrogen bonding interactions [59,60].

Much effort has been devoted to the design and synthesis of ligands capable of recognizing G,C-containing sequences through specific hydrogen bonding to the 2-amino group of guanine [61,62]. The present results suggest that GC/AT selectivity ratios can be increased by modulating the stacking properties of suitable intercalating moieties and taking full advantage of the sequence-dependent stacking characteristics of DNA base pairs.

Acknowledgements

We thank Dr. Ferrán Sanz for kindly providing the MEPSIM suite of programs. This research has been financed in part by the Spanish CICYT (Projects SAF94-0630 and SAF96-0231) and the University of Alcalá. J.G. was the recipient of a grant from the Spanish Ministerio de Educación y Ciencia (PN89-25126387), A.R.O. is a fellow of Comunidad de Madrid, and B.P.T. acknowledges financial support from Ministerio de Educación y Ciencia. Biosym Technologies Inc. (San Diego, CA, U.S.A.) contributed a software license.

References

1 Bailly, C. and Waring, M.J., Nucleic Acids Res., 23 (1995) 885.
2 Müller, W. and Crothers, D.M., J. Mol. Biol., 35 (1968) 251.
3 Van Dycke, M.W., Hertzberg, R.P. and Dervan, P.B., Proc. Natl. Acad. Sci. USA, 79 (1982) 5470.
4 Lane, M.J., Dabrowiak, J.C. and Vournakis, J.N., Proc. Natl. Acad. Sci. USA, 80 (1983) 3260.
5 Scamrov, A.V. and Beabealashvilli, R.Sh., FEBS Lett., 164 (1983) 97.
6 Fox, K.R. and Waring, M.J., Nucleic Acids Res., 12 (1984) 9271.
7 Waterloh, K. and Fox, K.R., Biochim. Biophys. Acta, 1131 (1992) 300.
8 Goodisman, J., Rehfuss, R., Ward, B. and Dabrowiak, J.C., Biochemistry, 31 (1992) 1046.
9 Snyder, J.G., Hartman, N.G., D'Estantoit, B.L., Kennard, O., Remeta, D.P. and Breslauer, K.J., Proc. Natl. Acad. Sci. USA, 86 (1989) 3968.
10 Bailey, S.A., Graves, D.E., Rill, R. and Marsch, G., Biochemistry, 32 (1993) 5881.

11 Bailey, S.A., Graves, D.E. and Rill, R., Biochemistry, 33 (1994) 11493.
12 Sobell, H.M., Jain, S.C., Sakore, T.D. and Nordman, C.E., Nat. New Biol., 231 (1971) 200.
13 Takusagawa, F., Dabrow, M., Neidle, S. and Berman, H.M., Nature, 296 (1982) 466.
14 Kamitori, S. and Takusagawa, F., J. Mol. Biol., 225 (1992) 445.
15 Kamitori, S. and Takusagawa, F., J. Am. Chem. Soc., 116 (1994) 4154.
16 Patel, D.J., Biochemistry, 13 (1974) 2396.
17 Lybrand, T.P., Brown, S.C., Creighton, S., Shafer, R.H. and Kollman, P.A., J. Mol. Biol., 191 (1986) 495.
18 Crothers, D.M. and Müller, W., Cancer Chemother. Rep., 58 (1974) 97.
19 Krugh, T.R., Mooberry, E.S. and Chiao, Y.-C.C., Biochemistry, 16 (1977) 740.
20 Chiao, Y.-C.C. and Krugh, T.R., Biochemistry, 16 (1977) 747.
21 Kopka, M.L., Goodsell, D.S., Baikalov, I., Grzeskowiak, K., Cascio, D. and Dickerson, R.E., Biochemistry, 33 (1994) 13593.
22 Cerami, A., Reich, E., Ward, D.C. and Goldberg, I.H., Proc. Natl. Acad. Sci. USA, 57 (1967) 1038.
23 Bailly, C., Marchand, C. and Waring, M.J., J. Am. Chem. Soc., 115 (1993) 3784.
24 Chen, F.-M., Biochemistry, 27 (1988) 6393.
25 Chen, F.-M., Biochemistry, 31 (1992) 6223.
26 Bernstein, F.C., Koetzle, T.F., Williams, G.J.B., Meyer Jr., E.F., Brice, M.D., Rodgers, J.R., Kennard, O., Shimanouchi, T. and Tasumi, M., J. Mol. Biol., 112 (1977) 535.
27 Ginell, S., Lessinger, L. and Berman, H.M., Biopolymers, 27 (1988) 843.
28 Gallego, J., Ph.D. Thesis, Universidad de Alcalá de Henares, Madrid, Spain, 1994.
29 AMBER, v. 4.0, Pearlman, D.A., Case, D.A., Caldwell, J., Seibel, G., Singh, U.C., Weiner, P. and Kollman, P.A., Department of Pharmaceutical Chemistry, University of California, San Francisco, CA, U.S.A., 1991.
30 Gago, F., Reynolds, C.A. and Richards, W.G., Mol. Pharmacol., 35 (1989) 232.
31 Gallego, J., Luque, F.J., Orozco, M., Burgos, C., Alvarez-Builla, J., Rodrigo, M.M. and Gago, F., J. Med. Chem., 37 (1994) 1602.
32 Jain, S.C. and Sobell, H.M., J. Mol. Biol., 68 (1972) 1.
33 Weiner, S.J., Kollman, P.A., Case, D.A., Singh, U.C., Ghio, C., Alagona, G., Profeta, S. and Weiner, P., J. Am. Chem. Soc., 106 (1984) 765.
34 Hopfinger, A.J. and Pearlstein, R.A., J. Comput. Chem., 5 (1984) 486.
35 Dewar, M.J.S., Zoebisch, E.G., Healy, E.F. and Stewart, J.J.P., J. Am. Chem. Soc., 107 (1985) 3902.
36 Chirlian, L.E. and Francl, M.M., J. Comput. Chem., 8 (1987) 894.
37 SPARTAN, v. 3.0.1, Wavefunction Inc., Irvine, CA, U.S.A., 1993.
38 Sanz, F., Manaut, F., Rodríguez, J., Lozoya, E. and López-de-Briñas, E., J. Comput.-Aided Mol. Design, 7 (1993) 337.
39 INSIGHT II, v. 2.3.0, Biosym Technologies, San Diego, CA, U.S.A., 1993.
40 Friedman, R.A. and Honig, B., Biopolymers, 32 (1992) 145.
41 Klapper, I., Hagstrom, R., Fine, R., Sharp, K. and Honig, B., Proteins, 1 (1986) 47.
42 Lee, B. and Richards, F.M., J. Mol. Biol., 55 (1971) 379.
43 Gilson, M.K., Sharp, K.A. and Honig, B., J. Comput. Chem., 9 (1988) 327.
44 Wold, S., Esbensen, K. and Geladi, P., Chemometr. Intell. Lab. Syst., 2 (1987) 37.
45 Wold, H., In David, F. (Ed.), Research Papers in Statistics, Wiley, New York, NY, U.S.A., 1966, pp. 411–444.
46 Boobyer, D.N.A., Goodford, P.J., McWhinnie, P.M. and Wade, R., J. Med. Chem., 32 (1989) 1083.
47 Gallego, J., de Pascual, B., Ortiz, A.R., Pisabarro, M.T. and Gago, F., In Sanz, F., Giraldo, J. and Manaut, F. (Eds.), QSAR and Molecular Modelling: Concepts, Computational Tools and Biological Applications, Prous Science, Barcelona, Spain, 1995, pp. 274–281.
48 Gallego, J., Ortiz, A.R. and Gago, F., J. Med. Chem., 36 (1993) 1548.
49 Lavery, R. and Pullman, B., Int. J. Quantum Chem., 20 (1981) 259.
50 Fox, K.R. and Waring, M.J., Eur. J. Biochem., 145 (1984) 579.
51 Bailly, C., Graves, D.E., Ridge, G. and Waring, M.J., Biochemistry, 33 (1994) 8736.
52 Dean, P.M. and Wakelin, L.P.G., Proc. R. Soc. London, B209 (1980) 473.
53 Wang, A.H.-J., Ughetto, G., Quigley, G.J., Hakoshima, T., Van der Marel, G.A., Van Boom, J.H. and Rich, A., Science, 225 (1984) 1115.
54 Marky, L.A., Snyder, J.G., Remeta, D.P. and Breslauer, K.J., J. Biomol. Struct. Dyn., 1 (1983) 487.
55 Quadrifoglio, F., Ciana, A. and Crescenzi, V., Biopolymers, 15 (1976) 595.
56 Gago, F. and Richards, W.G., Mol. Pharmacol., 37 (1990) 341.
57 Hunter, C.A., J. Mol. Biol., 230 (1993) 1025.
58 Gallego, J., Luque, F.J., Orozco, M. and Gago, F., J. Biomol. Struct. Dyn., 12 (1994) 111.
59 Krugh, T.R. and Reinhardt, C.G., J. Mol. Biol., 97 (1975) 133.
60 Müller, W. and Crothers, D.M., Eur. J. Biochem., 54 (1975) 267.
61 Cruciani, G. and Goodford, P.J., J. Mol. Graph., 12 (1994) 116.
62 Geierstanger, B.H., Mrksich, M., Dervan, P.B. and Wemmer, D.E., Science, 266 (1994) 646.